Simian Virus 40 Large T-Antigen G-Quadruplex DNA Helicase Inhibition by G-Quadruplex DNA-Interactive Agents†

Bodin Tuesuwan,‡ Jonathan T. Kern,§,|| Pei Wang Thomas,‡ Mireya Rodriguez,§ Jing Li,‡ Wendi M. David,⊥ and Sean M. Kerwin*,‡,§

Division of Medicinal Chemistry, College of Pharmacy, and Department of Chemistry and Biochemistry, The University of Texas at Austin, Austin, Texas 78712, and Department of Chemistry and Biochemistry, Texas State University, San Marcos, Texas 78666

Received August 28, 2007; Revised Manuscript Received November 28, 2007

ABSTRACT: On the basis of growing evidence for G-quadruplex DNA structures in genomic DNA and the presumed need to resolve these structures for DNA replication, the G-quadruplex DNA unwinding ability of a prototypical replicative helicase, SV40 large T-antigen (T-ag), was investigated. Here, we demonstrate that this G-quadruplex helicase activity is robust and comparable to the duplex helicase activity of T-ag. Analysis of the SV40 genome demonstrates the presence of sequences that may form intramolecular G-quadruplexes, which are the presumed natural substrates for the G-quadruplex helicase activity of T-ag. A number of G-quadruplex-interactive agents as well as new perylene diimide (PDI) derivatives have been investigated as inhibitors of both the G-quadruplex and the duplex DNA helicase activities of T-ag. A unique subset of these G-quadruplex-interactive agents inhibits the G-quadruplex DNA unwinding activity of T-ag, relative to those reported to inhibit G-quadruplex DNA unwinding by RecQ-family helicases. We also find that certain PDIs are both potent and selective inhibitors of the G-quadruplex DNA helicase activity of T-ag. Surface plasmon resonance and fluorescence spectroscopic G-quadruplex DNA binding studies of these T-ag G-quadruplex helicase inhibitors have been carried out, demonstrating the importance of attributes in addition to binding affinity for G-quadruplex DNA that may be important for inhibition. The identification of potent and selective inhibitors of the G-quadruplex helicase activity of T-ag provides tools for probing the specific role of this activity in SV40 replication.

The ability of G-rich DNA sequences to adopt G-quadruplex structures, even in the context of double-stranded DNA, is well-established in vitro (*1*−*5*). There are predictions of in excess of 370 000 putative quadruplex-forming sequences throughout the human genome (*6*, *7*). It has been suggested that there is a correlation between G-quadruplex formation and genetic stability (*8*−*10*) and gene function (*11*, *12*). Perhaps the strongest evidence for the formation of G-quadruplex DNA in cells comes from visualization by electron microscopy of G-loops, G-quadruplex DNA-containing structures formed on the nontemplate strand during transcription of G-rich DNA in *Escherichia coli* (*13*).

Evidence for a biological role of G-quadruplex DNA includes a growing list of proteins that display specific interactions with these higher-order DNA structures (*14*). Helicases in the RecQ family, including *E. coli* RecQ (*15*), Sgs1p (*16*), BLM (*17*), and WRN (*18*) have been shown to possess G-quadruplex unwinding ability. These RecQ-family helicases share a C-terminal G-quadruplex binding domain, RQC (*19*). While it has been hypothesized that the G-quadruplex unwinding activity of these RecQ helicases is required to resolve structures that form throughout the genome during DNA replication and recombination (*19*), the exact biological role for the G-quadruplex DNA unwinding activity of these RecQ helicases is not known.

To date, few non-RecQ-family helicases have been shown to unwind G-quadruplex DNA structures (*20*). SV40 large T-antigen (T-ag[1]) is a multifunctional protein required for viral replication and transformation whose functions include double-stranded DNA helicase activity (*21*). The replication of the SV40 genome has many biochemical similarities to that of eukaryotic chromosomes and is often employed as a model system for studying cellular DNA replication (*22*−*24*). In addition to its duplex DNA helicase activity, T-ag has also been reported to unwind G-quadruplex structures (*25*). The role for this G-quadruplex helicase activity in SV40 replication has not been determined, but an unusual four-stranded G-quadruplex has been observed by NMR for an oligonucleotide encompassing a GGGCGG repeat sequence

† This publication was supported by Grants 5 P30 ES07784 and RO1 GM65956 from the NIH and F-1298 from the Robert A. Welch Foundation.

* Corresponding author. Tel.: (512) 471-5074. Fax: (512) 232-2606. E-mail: skerwin@mail.utexas.edu.

‡ Division of Medicinal Chemistry, College of Pharmacy, The University of Texas at Austin.

§ Department of Chemistry and Biochemistry, The University of Texas at Austin.

|| Current address: Department of Movement Disorders, Merck Research Laboratories, West Point, PA 19486.

⊥ Texas State University.

[1] Abbreviations: BSA, bovine serum albumin; Dist, distamycin A; DMSO, dimethyl sulfoxide; DTT, dithiothreitol; EDTA, *N*,*N*,*N*′,*N*′-ethylenediaminetetraacetic acid; PAGE, polyacrylamide gel electrophoresis; PDI, 3,4,9,10-perylenetetracarboxylic acid diimide; QGRS, quadruplex-forming G-rich sequence; RQC, RecQ C-terminal domain; SDS, sodium dodecyl sulfate; SPR, surface plasmon resonance; SV40, simian virus 40; T-ag, large T-antigen; Tris, *N*,*N*,*N*-tris(hydroxymethyl)-aminomethane.

10.1021/bi701747d CCC: $40.75
Published on Web 01/19/2008

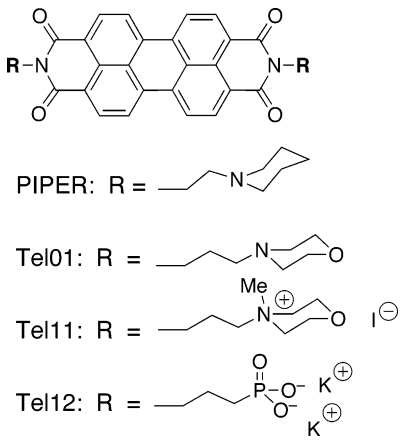

FIGURE 1: Examples of perylene diimide G-quadruplex-interactive agents.

in the SV40 genome (*26*). Interestingly, certain antiproliferative G-rich oligonucleotides (GROs), which can form dimeric or monomeric G-quadruplex structures (*27*), have been shown to inhibit T-ag duplex helicase activity (*28*). Given the kinetic stability of G-quadruplex DNA (*29*) and the ability of G-quadruplex structures to serve as efficient blocks to DNA polymerization (*30*), the ability of hexameric helicases such as T-ag to unwind these structures may be a general requirement for efficient DNA replication.

One promising class of quadruplex selective ligands is perylene diimides (PDIs) (Figure 1) (*31*−*37*). Recent NMR studies of *N*,*N*′-bis[2-(1-piperidino)-ethyl]-3,4,9,10-perylenetetracarboxylic acid diimide (PIPER) (*31*) and *N*,*N*′-bis-(4-morpholinylpropyl)-3,4,9,10-perylenetetracarboxylic acid diimide (Tel01) (*38*) (Figure 1) indicate that these molecules bind to G-quadruplex DNA by stacking on the faces of the terminal G-tetrads, thereby stabilizing the G-quadruplex structure. Interestingly, the selectivity of these ligands for G-quadruplex DNA versus duplex DNA can be quite high, particularly under conditions where the ligands form aggregates (*38*, *39*).

The potential of G-quadruplex DNA-interactive agents to interfere with G-quadruplex DNA helicases such as those of the RecQ family has been recognized as a potential therapeutic approach (*40*). Inhibition of G-quadruplex helicases involved in telomere maintenance by telomerase or telomerase-independent (ALT) pathways may provide a means of limiting the replicative capacity of cancer cells. Alternatively, inhibiting the helicase unwinding of G-quadruplex structures formed in oncogene promoters may result in transcriptional down-regulation of these genes. While a number of G-quadruplex-interactive ligands have been reported to inhibit the G-quadruplex unwinding activity of RecQ helicases, issues of selectivity remain. The cationic porphyrin TMPyP4 (Figure 2) inhibits the G-quadruplex helicase activity of *E. coli* RecQ (*8*), yeast Sgs1 (*41*), and human BLM (*41*, *42*) and WRN (*42*) helicases, although the inhibition is generally not selective for G-quadruplex versus duplex DNA. In contrast, the anionic porphyrin NMM (Figure 2) is a specific inhibitor of the G-quadruplex helicase activity of RecQ (*8*), BLM (*41*, *43*), and Sgs1 (*41*). The PDI PIPER (Figure 1) is also a potent and selective inhibitor of Sgs1 (*44*). However, the molecular features of G-quadruplex-interactive agents that give rise to potent and selective RecQ G-quadruplex helicase inhibition are not well-established. Distamycin (Figure 2), which binds to G-quadruplex DNA, does not inhibit the G-quadruplex helicase activity of BLM, although it does prevent duplex unwinding by this enzyme (*43*).

Unlike these studies of the RecQ helicases, there have been no studies on the effects of G-quadruplex DNA-interactive agents on T-ag G-quadruplex helicase activity. Studies of the effect of a variety of G-quadruplex-interactive agents on different G-quadruplex helicases will lead to a better understanding of the structural basis for selective targeting of different families of G-quadruplex DNA helicases. Inhibitors of specific classes of G-quadruplex helicases may be useful as tools to elucidate the role of G-quadruplex unwinding in specific biological processes or as therapeutic agents targeting these processes.

Here, we confirm and expand upon the previous report of T-ag G-quadruplex helicase activity. We demonstrate that this G-quadruplex helicase activity is efficient as compared to the duplex helicase activity of T-ag. Analysis of the SV40 genome demonstrates the presence of sequences that may form intramolecular G-quadruplexes, which are the presumed natural substrates for the G-quadruplex helicase activity of T-ag. A number of G-quadruplex-interactive agents as well as new PDI derivatives have been investigated as inhibitors of both the G-quadruplex and the duplex DNA helicase activities of T-ag. We find that a unique subset of these G-quadruplex-interactive agents inhibit the G-quadruplex DNA unwinding activity of T-ag, relative to those reported to inhibit G-quadruplex DNA unwinding by RecQ-family helicases. We also find that certain PDIs are both potent and selective inhibitors of the G-quadruplex DNA helicase activity of T-ag. Binding studies of these T-ag G-quadruplex helicase inhibitors have been carried out. These studies indicate that in addition to binding affinity, other aspects of G-quadruplex-interactive agents may be important for effective inhibition of the T-ag G-quadruplex helicase.

EXPERIMENTAL PROCEDURES

Unless otherwise noted, all materials were obtained from commercial suppliers and used without further purification. SV40 T-ag prepared in insect cells was obtained commercially from CHIMERx or as a kind gift from Dr. Daniel T. Simmons, University of Delaware.

DNA Preparation. The following deoxyoligonucleotides were used in the studies: *DNA1*, TTG GGG TTG GGG CTA CGC GAT CAG; *DNA2*, GAG CAG CAA TAC ACG A; and *DNA3*, TCG TGT ATT GCT GCT CTC TCT CTC TC. DNA1 and DNA2 (2.25 nmol) were 5′-labeled with [γ-^{32}P] ATP using T4 polynucleotide kinase. After the kinase reaction was stopped, 1 μL of the reaction was archived, and the rest was purified by elution through a Biospin column. The formation of DNA1-G′2 was performed as described (*25*). Briefly, the radiolabeled DNA1 was dissolved in TE buffer (0.5 μM), heated for 5 min at 95 °C, and rapidly cooled in ice. Then, KCl was added to a final concentration of 0.3 M, and the solution was heated at 45 °C in a water bath and annealed for 40−45 h. DNA1-G4 was formed similarly by replacing the KCl with NaCl (0.5 M). Duplex DNA was formed by annealing 5′-radiolabeled DNA2 and nonlabeled DNA3 at a 1:3 ratio in TE buffer. The mixture was heated at 95 °C for 5 min and slowly cooled to room

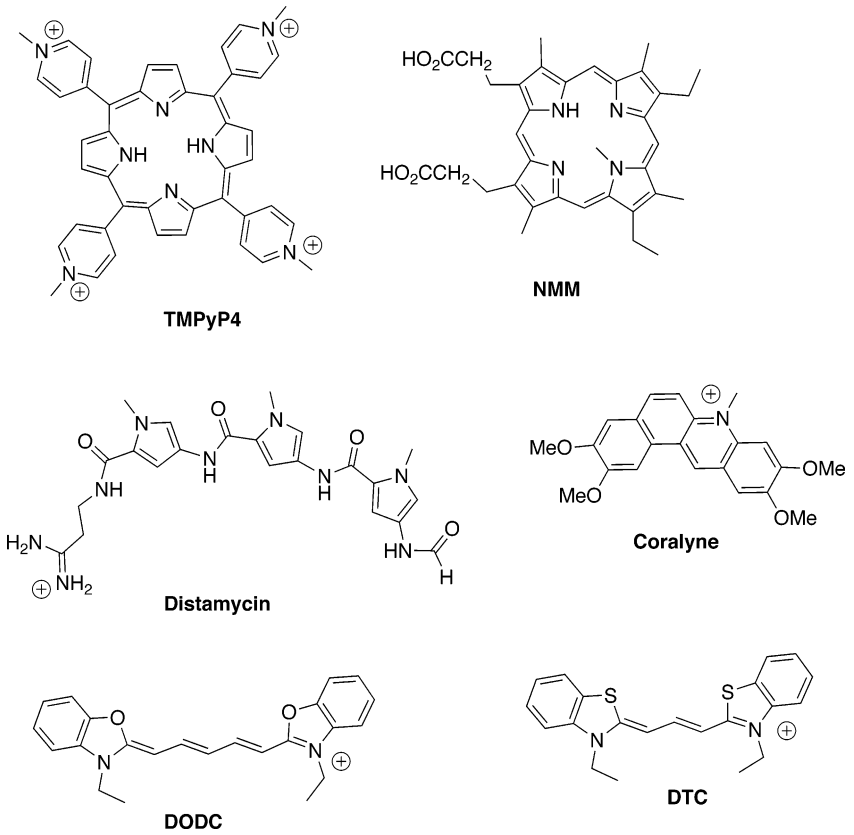

FIGURE 2: Structures of other G-quadruplex-interactive agents examined for T-ag helicase inhibition.

temperature for approximately 16 h. All annealed DNA samples were purified by 12% nondenaturing polyacrylamide electrophoresis and eluted in buffer prior to use. To determine the concentration of the purified G-quadruplex DNA and double-stranded DNA, samples of each were subjected to PAGE along with the archived, unpurified sample. Using the known concentration of the DNA in the archived sample, the DNA concentration in the purified, annealed samples was determined by the ratio of the band intensities determined by phosphorimaging.

Helicase Assay. Helicase assays were carried out in 10 μL of a solution containing 10 mM Tris-HCl buffer (pH 7), 10 mM KCl, 10 mM $MgCl_2$, 0.5 mM 1,4-dithiothreitol, 50 μg/μL BSA, 2 mM ATP, 0.1 mM EDTA, 10% glycerol, ^{32}P-labeled DNA substrate (0.38 pmol), and SV40 large T-ag (0.2−0.85 μg of protein). The reactions were performed at 37 °C for 90 min. The reactions were terminated by adding a stop solution that contained 15% glycerol, 3% SDS, 20 mM EDTA, 8 mM Tris-HCl, pH 8, 0.8 mM bromphenol blue, and 1 mM xylene cyanol and, in the case of duplex unwinding assays, 1.14 pmol of unlabeled DNA2. The reaction products were separated by electrophoresis in 12% nondenaturing polyacrylamide gels.

Fluorescence Spectroscopy. Spectra were recorded on a Hitachi model F-2000 spectrofluorometer in silanized quartz cuvettes or on a Beckman Coulter model DTX 800 plate reader using black polystyrene 384-well microplates (Nunc). The compounds (1 μM) and various concentrations of G′2-DNA or ds-DNA2/3 were mixed in a buffer containing 10 mM Tris-HCl buffer (pH 7), 10 mM KCl, 10 mM $MgCl_2$, 0.5 mM 1,4-dithiothreitol, 0.1 mM EDTA, and 10% glycerol. The solutions were allowed to equilibrate, and their fluorescence was measured. Dissociation constants were determined by nonlinear least-squares fitting of the increase or decrease of fluorescence due to ligand binding using the procedure described by Aldrich-Wright et al. (*45*). Briefly, the equilibrium dissociation constant (K_d) is expressed as

$$K_d = [L_T - L_B][S_T - L_B]/[L_B] \quad (1)$$

where L_B is the concentration of bound ligand complex sites, and L_T and S_T are the total concentrations of ligand and DNA binding sites, respectively.

The amount of complex formed is proportional to the change in fluorescence according to the following equation:

$$L_B = (\Delta F/\Delta F_{max})L_T \quad (2)$$

where ΔF is the increase or decrease in fluorescence upon addition of each DNA concentration, and ΔF_{max} is the maximum change in fluorescence at saturating conditions.

Combining eqs 1 and 2 affords the quadratic equation (eq 3)

$$L_T(\Delta F/\Delta F_{max})^2 - (L_T + S_T + K_d)(\Delta F/\Delta F_{max}) + S_T = 0 \quad (3)$$

Solving for the root of the quadratic equation (eq 3) leads to

$$\Delta F/\Delta F_{max} = ((L_T + S_T + K_d) - ((((L_T + S_T + K_d)^2) - (4L_TS_T))^{1/2}))/(2L_T) \quad (4)$$

The change in fluorescence, $\Delta F/\Delta F_{max}$, determined experimentally was plotted against the total number of binding sites, S_T, which is equal to the total concentration of DNA

Scheme 1: Synthesis of Chromophore-Modified PDIs

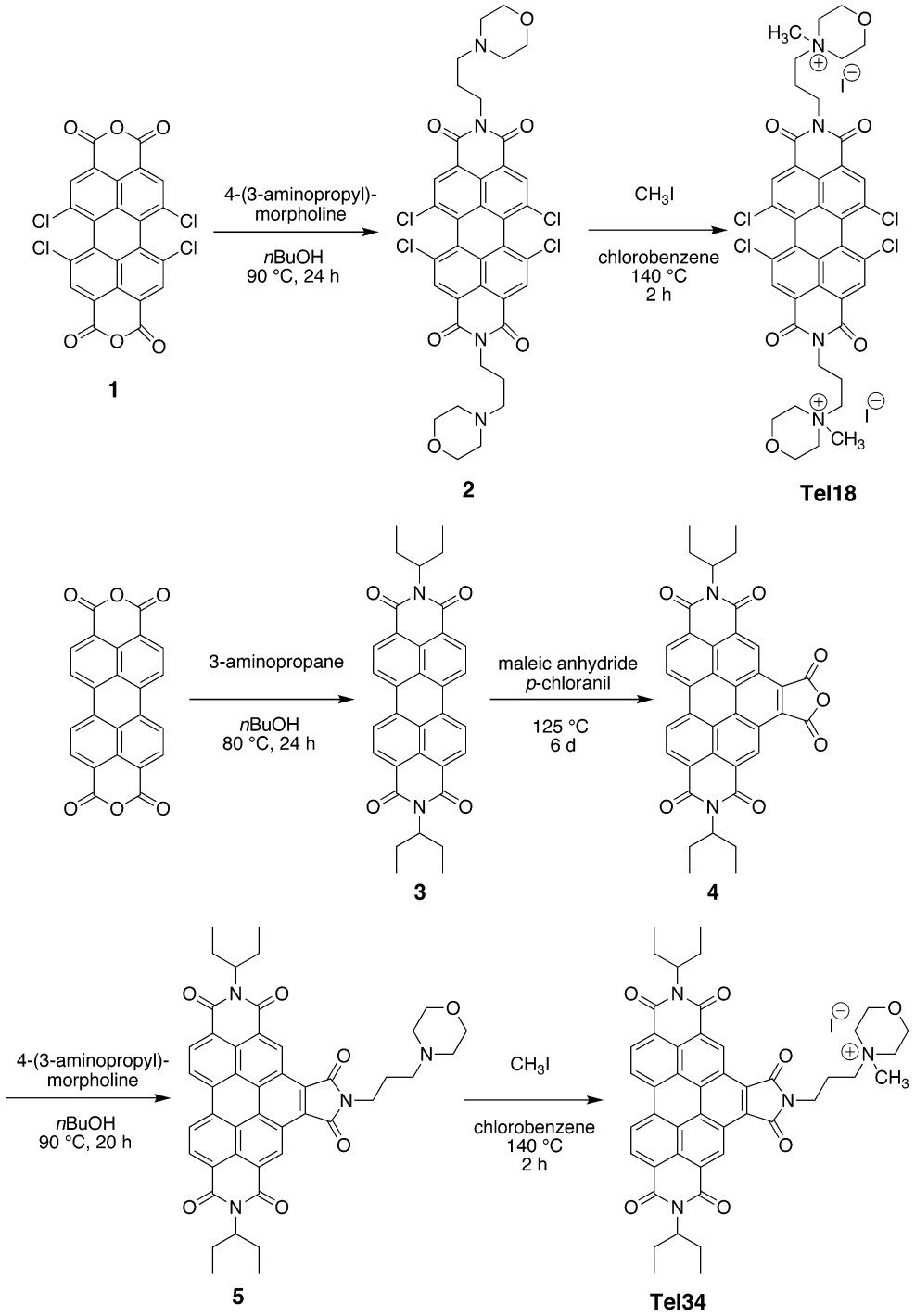

multiplied by the number of binding sites per structure. The number of binding sites per DNA structure (n) was determined by substituting $S_T = DNA_T n$ in eqs 3 and 4.

Surface Plasmon Resonance. The SPR experiments were performed using a Biacore X optical biosensor system with streptavidin-coated sensor chips (GE Healthcare). Sensor chips were derivatized on one flow channel with low levels (~200 RU (response units)) of 5′-biotinylated DNA (5′ BioTEG-$(TTAGGG)_4$TT, Integrated DNA Technologies) in filtered and degassed HBS-EP buffer (0.01 M HEPES, pH 7.4, 0.15 M NaCl, 3 mM EDTA, and 0.005% v/v P20 surfactant) after several preconditioning injections of 1 M NaCl/50 mM NaOH. To facilitate and maintain the formation of the intramolecular G-quadruplex DNA, the HBS-EP buffer containing 200 mM KCl was subsequently used both as a running buffer and as a storage buffer for derivatized sensor chips. Formation of the G-quadruplex was verified by the inability of the derivatized chips to bind *E. coli* single-strand binding protein (Sigma-Aldrich) under the conditions used for binding experiments. TMPyP4 and Tel11 were dissolved in running buffer (HBS-EP buffer containing 200 mM KCl) and injected manually (50 μL) at different concentrations using a flow rate of 10 μL/min to allow long contact times. Binding profiles at this flow rate were determined to be the same as observed at higher flow rates (20 μL/min), indicating the absence of significant mass transport effects. Injections

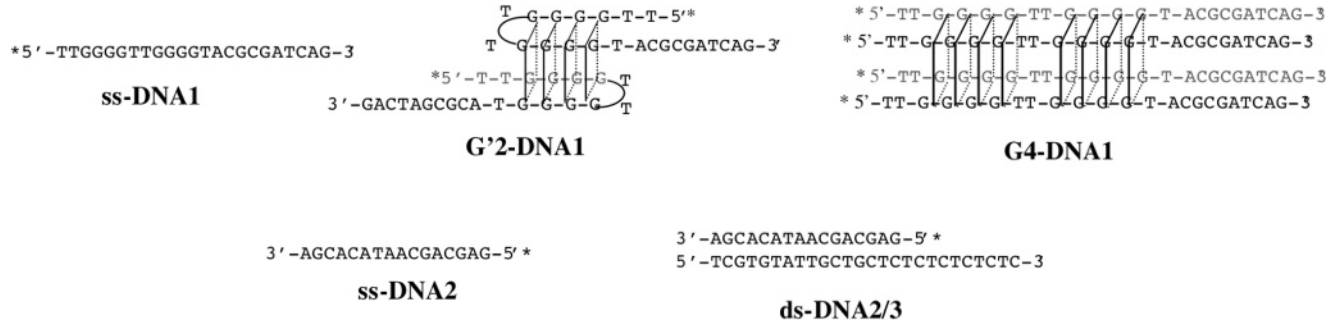

FIGURE 3: DNA structures used in these studies.

were followed by a dissociation period of 7 min (running buffer, 10 μL/min) and subsequent alternating injections of running buffer, 5% DMSO, and 1% P20 to wash the flow cells. The experiments were performed in multichannel mode using a control flow cell that was not derivatized with DNA. All binding responses were determined relative to the control flow cell. Fitting of steady-state equilibrium binding constants and kinetic association and dissociation curves was performed using BIAevaluation software supplied with the Biacore X instrument.

RESULTS AND DISCUSSION

Synthesis of Chromophore-Modified PDIs. To have a more diverse group of G-quadruplex-interactive agents to explore T-ag helicase inhibition structure−activity relationships, two new chromophore-modified PDIs were prepared. Effects of modifications to the PDI chromophore, as in Tel18 and Tel34 (Scheme 1), on G-quadruplex DNA binding have not been widely explored (*46*, *47*). The addition of halogen atoms to the bay positions of the perylene chromophore, as in Tel18 (Scheme 1), has been reported to decrease the ligands' tendency for self-association, presumably as a result of the twist that these substituents induce into the otherwise planar PDI chromophore (*48*, *49*). Benzannulation of the PDI chromophore, as in Tel34 (Scheme 1), may enhance the $\pi-\pi$ stacking between the ligand and the face of the G-tetrad.

The preparation of tetrachlorinated PDI Tel18 followed that of the previously reported nonhalogenated analogue Tel11 (Figure 1) but proceeded from the commercially available 1,6,7,12-tetrachloro-3,4,9,10-tetracarboxylic dianhydride (**1**, Scheme 1). Langhals and Kirner reported the preparation of benzannulated perylene diimides via Diels−Alder cycloaddition of perylene diimides in molten maleic anhydride in the presence of *p*-chloranil (*50*). Following this route, the anhydride **4** was prepared from the PDI **3** (Scheme 1). The reactivity and rather limited solubility of anhydride **4** made characterization of this intermediate difficult; however, its structure was inferred from the formation of the corresponding triimide in 75% yield in the presence of 3-aminopentane. Condensation of **4** with 4-(3-aminopropyl)-morpholine afforded the triimide **5** in 71% yield. Methylation of **5** with excess methyl iodide in chlorobenzene gave Tel34 in 98% yield. Experimental details and compound characterization data are provided in the Supporting Information.

Preparation of DNA Substrates. A 5′-radiolabeled DNA oligonucleotide (DNA1, Figure 3) containing two TTGGGG repeats was annealed in a K^+ ion-containing buffer to form predominantly the bimolecular G-quadruplex structure (G′2-DNA), which was purified by preparative polyacrylamide gel electrophoresis. In addition to its altered gel mobility, this structure was characterized by DMS protection, which demonstrated reduced accessibility of the Gs in the TTGGG repeats relative to unfolded DNA1 (Supporting Information). While the structure of the bimolecular-DNA1 G-quadruplex shown in Figure 3 is of a head-to-tail type with lateral loops on opposite ends of the G-tetrad stack, our characterization was not able to distinguish this form from alternative possible structures including head-to-head or basket-type dimers. Annealing the same DNA1 oligonucleotide in Na^+ ion-containing buffer afforded the tetramolecular-DNA1 G-quadruplex (G4-DNA, Figure 3), which was also purified by preparative electrophoresis and characterized by DMS protection of the Gs forming the G-tetrads. A duplex helicase substrate containing a 3′-single-stranded tail (ds-DNA2/3) was prepared by annealing 5′-radiolabeled oligonucleotide DNA2 with a complementary strand containing an oligo-CT tail (DNA3) (Figure 3).

T-ag Unwinds a G-Quadruplex Substrate Better Than a Duplex DNA Substrate. On the basis of the work of Manor and co-workers (*25*), we explored the selectivity of SV40 T-ag helicase activity employing bimolecular-DNA1 and duplex DNA substrates. These substrates allow the progress of the unwinding reactions to be monitored by nondenaturing PAGE, as the single-stranded DNA product is easily separated from duplex or G-quadruplex substrates (*51*).

In the presence of Mg^{2+} and ATP (4 mM) in a 10 mM NaCl-containing buffer, commercially available T-ag efficiently unwinds the bimolecular-DNA1 G-quadruplex substrate (Supporting Information). The tetramolecular DNA1 quadruplex is also unwound; however, in this case, the extent of unwinding is greater in the NaCl-containing buffer than in the KCl-containing buffer (Supporting Information). The T-ag unwinding of these G-quadruplex substrates requires ATP and does not occur in the presence on the nonhydrolyzable ATP analogue AMP-PNP (data not shown).

While the duplex DNA unwinding activity of T-ag is well-established, in our hands, commercially available T-ag converts the duplex ds-DNA2/3 substrate to single-stranded DNA2 and an additional, higher-mobility product (Supporting Information). Comparison of the duplex versus bimolecular-DNA1 G-quadruplex unwinding efficiency of commercial T-ag indicates that the quadruplex is unwound at least as efficiently as the duplex substrate; however, the presence of an apparent nuclease cleavage of the duplex substrate under these conditions makes this comparison difficult.

A better comparison of the duplex versus bimolecular G-quadruplex unwinding activity of T-ag was obtained using

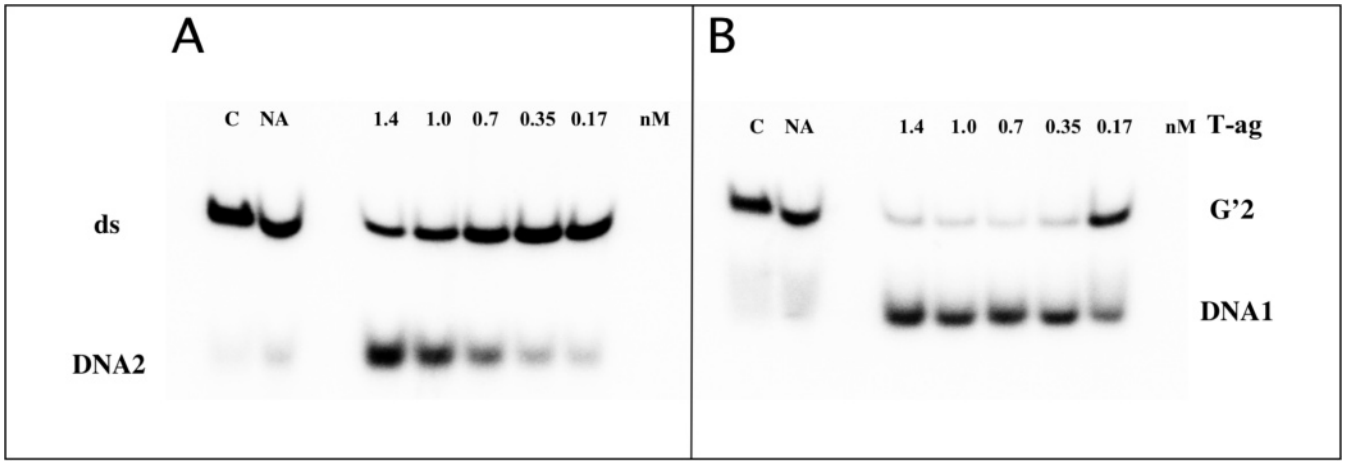

FIGURE 4: Comparison of duplex and G-quadruplex DNA helicase activity of T-ag. Incubation of 0.38 pmol of 5′-labeled ds-DNA2/3 (A) or G′2-DNA1 (B) was carried out with the indicated concentration of recombinant, immunopurified T-ag and 4 mM ATP for 90 min at 37 °C in 10 mM Tris-HCl, 10 mM KCl, 10 mM $MgCl_2$, 0.5 mM DTT, 50 μg/μL BSA, 0.1 mM EDTA, and 10% glycerol at pH 7. The reaction products were analyzed by nondenaturing gel electrophoresis. Lanes C are DNA substrate in the absence of T-ag, and lanes NA are the substrate in the presence of T-ag but without added ATP.

noncommercial immunochromatography-purified recombinant T-ag expressed in insect cells (*52*). This source of T-ag did not display the apparent nuclease activity associated with the commercially available material. In the presence of increasing concentrations of this T-ag, the duplex ds-DNA2/3 substrate is unwound to single-stranded DNA2 in an ATP-dependent fashion without the production of higher-mobility products (Figure 4A). However, under these conditions, the concentration of T-ag required for unwinding of the duplex DNA substrate is 6−8-fold higher than that required for unwinding the bimolecular G-quadruplex substrate (Figure 4B). This preference for unwinding G-quadruplex DNA was also observed at other time points during the course of the helicase reaction (Supporting Information); however, it is possible that the difference in unwinding efficiency measured under these conditions is due, in part, to the faster reannealing of the duplex substrate after the helicase unwinding. Although RecQ-family helicases prefer G-quadruplex to duplex substrates (*19*), recBCD only unwinds the duplex ds-DNA2/3 and not the bimolecular-DNA1 G-quadruplex substrate (data not shown). The concentration of T-ag required to completely unwind the bimolecular quadruplex substrate under these conditions (0.35 nM T-ag hexamer) is 100 times lower than the approximate substrate concentration in these assays (38 nM), further illustrating the efficiency of the G-quadruplex helicase activity of T-ag.

These studies confirm and expand upon the earlier report by Manor and co-workers of the G-quadruplex helicase activity of T-ag (*25*). It is shown that T-ag unwinds bimolecular G-quadruplex DNA with high efficiency. The RecQ-family helicases, which also unwind G-quadruplex DNA, possess a RQC G-quadruplex DNA binding motif. SV40 T-ag does not possess a RQC domain or any other previously reported G-quadruplex DNA-interactive protein motif. Thus, the mode of interaction of T-ag with G-quadruplex DNA may be distinct from that for RecQ-family helicases and other G-quadruplex-associated proteins.

Potential Intramolecular G-Quadruplex DNA Structures in SV40 DNA. The demonstration of a robust bimolecular G-quadruplex unwinding activity of SV40 T-ag led to an investigation of the potential G-quadruplex structures in the SV40 genome. NMR analysis of d(TGGCGG), an oligonucleotide incorporating an SV40 5′-GGGCGG-3′ repeat (*26*), demonstrates the formation of an unusual tetramolecular G-quadruplex containing a C-tetrad sandwiched between adjacent G-tetrad stacks. However, no prior work has explored the potential for intramolecular G-quadruplex structures in SV40 DNA. Such intramolecular quadruplexes could form even in the context of the double-stranded DNA sequences (*2*−*4*), particularly during processes in which the strands are transiently separated (*11*) or under superhelical stress (*53*), such as occurs during DNA replication. A number of algorithms have been proposed to identify putative intramolecular G-quadruplex-forming regions in DNA and RNA (*6*, *7*, *11*, *54*). The QGRS Mapper algorithm is available online and is representative of other approaches in that it searches user-defined windows of sequence for four runs of two or more consecutive Gs separated by loops of intervening bases that can vary from zero up to a user-defined maximal loop length (*55*).

Employing QGRS Mapper, a number of putative intramolecular G-quadruplex DNA-forming regions were identified in the SV40 genome. The location of these regions on the SV40 genome is shown in Figure 5, and the sequences are provided in the Supporting Information. These potential G-quadruplex-forming regions are not uniformly distributed throughout the SV40 genome but rather occur primarily near the origin of replication and adjacent to the polyadenylation signals for the early and late transcripts. There is a strong strand bias for the location of the remaining potential G-quadruplex-forming regions, which are distributed on the coding strand, most notably on the early transcripts.

The results of the search for potential G-quadruplex-forming regions were relatively insensitive to the search parameters of sequence window and loop size; however, the results were very dependent on the minimum number of G-tetrads allowed. The results discussed previously were derived from searches in which the minimum number of G-tetrads was two; changing this parameter to three resulted in the identification of a single potential G-quadruplex structure in SV40. This presumably more robust potential G-quadruplex encompasses the 21-base-pair repeat region

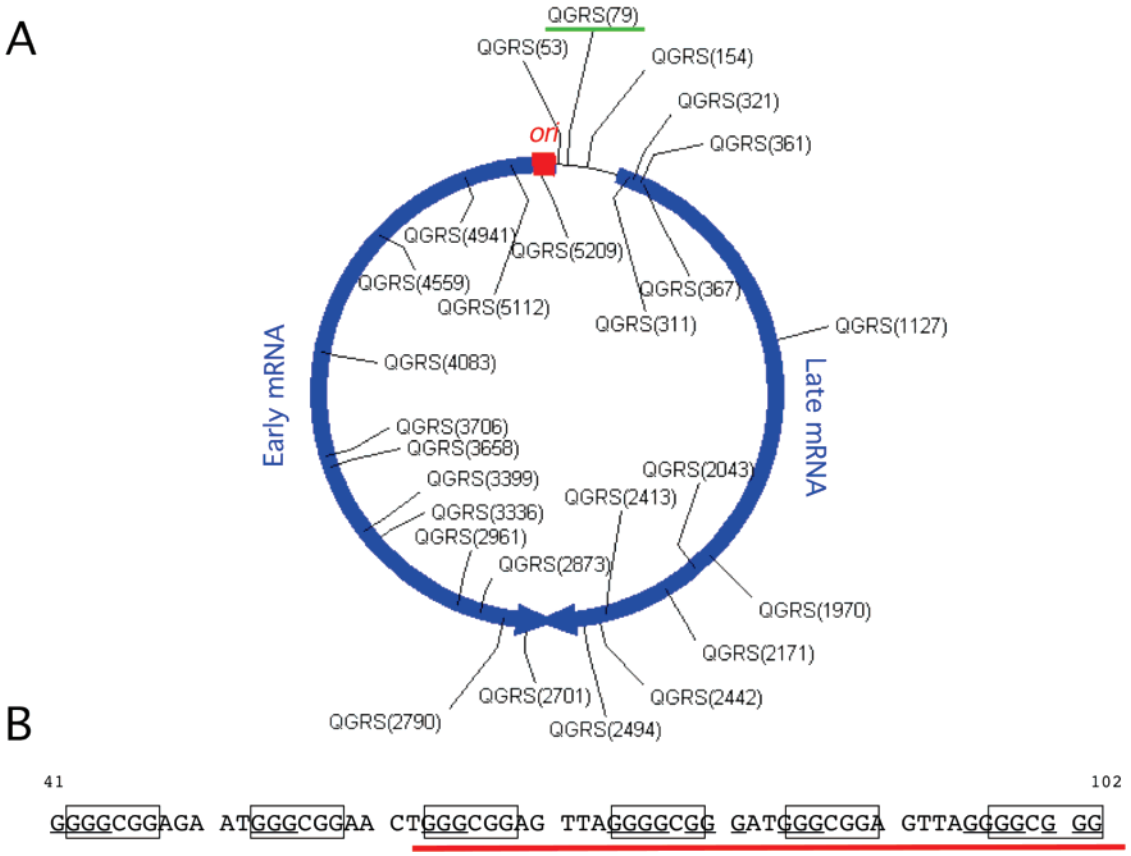

FIGURE 5: (A) Map of SV40 genome showing the location of potential G-quadruplex-forming G-rich sequences (QGRS). The QGRS were identified using as search parameters the following: maximum length 30, minimum G-group size 2, and loop size from 0 to 22. (B) Detail of the QGRS at position 79 (underlined in panel A). Each run of three Gs is underlined, the multiple GGGCGG repeats are boxed, and the 21-bp repeat is denoted by a red line under the sequence. The numbers on top of the sequence signify the position, based on NCBI reference sequence NC_001669.

of SV40, which plays an important role in both viral transcription and replication and contains binding sites for many proteins including Sp1 (*56*). It consists of multiple runs of three consecutive Gs, such that multiple potential G-quadruplex structures may form. Interestingly, this region also encompasses six GGGCGG repeats, which are highlighted in Figure 5B. Assuming a similar arrangement of mixed G- and C-tetrads as observed in the tetramolecular G-quadruplex incorporating this sequence can be formed in intramolecular quadruplexes, this QGRS from SV40 could adopt multiple such quadruplexes with loop sizes ranging from three to five nucleotides.

The potential G-quadruplex-forming region occurs close to the origin of replication. To the extent that this or the other potential G-quadruplex-forming regions in SV40 fold into intramolecular DNA G-quadruplex structures, they could hinder the replication of the viral DNA in the absence of a means to unfold these structures. Provided that SV40 T-ag also possesses intramolecular G-quadruplex helicase activity in addition to the bimolecular G-quadruplex helicase activity shown here, T-ag could provide such a means to resolve these structures to allow unimpeded DNA synthesis.

G-Quadruplex DNA-Interactive Agents Inhibit T-ag G-Quadruplex Helicase Activity. To explore the nature of the interaction of T-ag with G-quadruplex substrates, a series of previously reported G-quadruplex-interactive agents was assayed for their ability to inhibit the G-quadruplex unwinding ability of T-ag. The anionic *N*-methyl mesoporphyrin (NMM) inhibits the G-quadruplex unwinding ability of T-ag with an IC_{50} value of 95 μM (Figure 6 and Table 1). This inhibition of the G-quadruplex unwinding activity of T-ag by NMM is similar to but less effective than the inhibitory effect of NMM on the quadruplex unwinding activity of RecQ, Sgs1, BLM, and WRN (*15*, *41*). In contrast, the cationic porphyrin TMPyP4, which has been shown to be a submicromolar inhibitor of quadruplex unwinding activity of the RecQ-family helicases BLM (*41*, *42*), WRN (*42*), Sgs1 (*41*, *57*), and RecQ (*15*), does not inhibit the quadruplex unwinding activity of T-ag, even at concentrations as high as 100 μM (Table 1). While other G-quadruplex-interactive agents have IC_{50} values >100 μM, they do display some inhibition of the bimolecular quadruplex unwinding by T-ag at 100 μM concentration (Figure 6). Distamycin A, which has been reported not to inhibit the quadruplex unwinding activity of BLM, is a weak inhibitor of the quadruplex unwinding activity of T-ag (Table 1). The carbocyanine DODC was originally reported as a G′2-specific ligand with a novel binding mode involving interactions with the groove and loops of these quadruplexes (*58*, *59*). DODC weakly inhibits the G′2 unwinding activity of T-ag (Figure 6 and Table 1). Coralyne, a recently reported selective G-quadruplex ligand and telomerase inhibitor (*60*), also weakly inhibits the quadruplex unwinding activity of T-ag.

A number of other G-quadruplex ligands are not effective inhibitors of the quadruplex unwinding activity of T-ag. Hoechst 33258 (*61*) and DTC (*39*, *62*) have been proposed to bind to G-quadruplex structures through groove or loop interactions. While Hoechst 33258 can inhibit the duplex

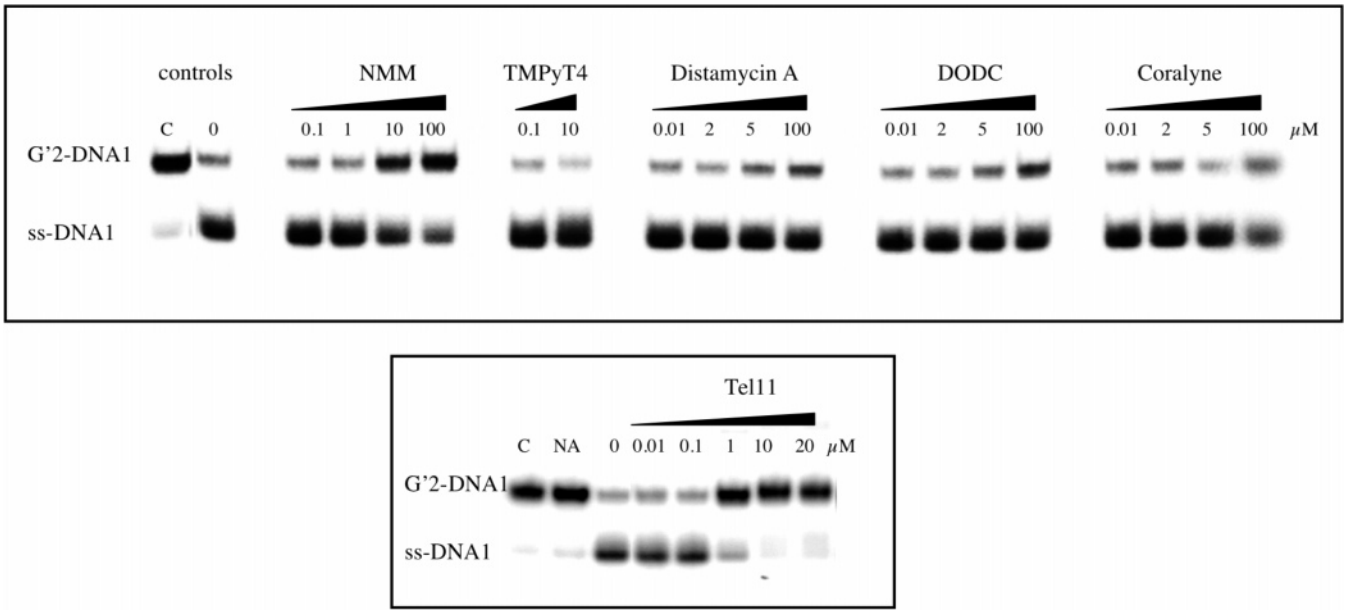

FIGURE 6: Inhibition of the G-quadruplex DNA helicase activity of T-ag by selected G-quadruplex-interactive agents. Each ligand was incubated with 5′-labeled G′2-DNA1 in helicase buffer for 60 min prior to the addition of 0.2 μg of recombinant, immunopurified T-ag and 4 mM ATP. After 90 min at 37 °C, the reactions were stopped, and the products were analyzed by nondenaturing gel electrophoresis. Lanes are labeled with the final concentration of ligand. The control lanes C are DNA in the absence of both ligand and T-ag, lane NA is the substrate DNA in the presence of T-ag but without added ATP, and lane 0 is DNA in the presence of T-ag and ATP with no added ligand.

Table 1: SV40 T-ag G′2 DNA Helicase Inhibition by G-Quadruplex DNA-Interactive Agents

compound	IC_{50} for T-ag G2-DNA1 unwinding (μM)
NMM	95 ± 5
TMPyP4	>100[a]
Dist	>100[b]
DODC	>100[c]
coralyne	>100[d]
Tel01	0.22 ± 0.06
PIPER	0.16 ± 0.02
Tel11	0.13 ± 0.06
Tel12	50 ± 9
Tel18	35 ± 2
Tel34	5 ± 4

[a] 0% inhibition at 100 μM. [b] 16% inhibition at 100 μM. [c] 24% inhibition at 100 μM. [d] 29% inhibition at 100 μM.

helicase activity of WRN and BLM (*63*), neither this compound nor DTC is an effective inhibitor of the quadruplex unwinding activity of T-ag (less than 15% inhibition at 10 μM, data not shown). Berberine, structurally related to coralyne, displays a diminished G-quadruplex DNA binding ability and telomerase inhibition (*60*) and is not an effective inhibitor of the quadruplex unwinding activity of T-ag (data not shown). Duplex DNA intercalators that have also been reported to bind to G-quadruplex DNA, such as TOTA (*64*) and ethidium bromide (*65*, *66*), are also not effective inhibitors of T-ag G-quadruplex DNA helicase activity. However, ethidium bromide has been reported to inhibit the duplex unwinding activity of T-ag (*67*).

From this study of G-quadruplex-interactive agents, two points can be made. First, the ability of these compounds to inhibit the G-quadruplex DNA helicase activity of T-ag does not correlate with the reported binding mode of these ligands for G-quadruplex structures. Both compounds that have been reported to end-stack on G-quadruplex DNA (NMM, coralyne) and those that have been reported to interact with loops or grooves of these structures (distamycin A, DODC) are inhibitors of the G-quadruplex helicase activity of T-ag. At the same time, there are also examples of both end-stackers (TMPyP4, TOTA, and ethidium bromide) and groove/loop binders (DTC, Hoechst 33258) that do not inhibit the quadruplex unwinding activity of T-ag. This lack of correlation between the reported G-quadruplex DNA binding mode for these ligands and their ability to inhibit the G-quadruplex unwinding ability of T-ag may be due to the uncertainties associated with the precise G-quadruplex binding mode(s) for these ligands. For example, distamycin has been reported to bind to G-quadruplex DNA through interactions with the G-quadruplex grooves (*68*) and by end-stacking on G-tetrad faces (*41*). For this and the other ligands examined here, the precise nature of the interaction with G-quadruplex DNA may be a function of the specific G-quadruplex structure.

A second observation from these studies is that the G-quadruplex-interactive agents that inhibit T-ag are different from those that inhibit the RecQ-family G-quadruplex helicases and vice versa. The range of G-quadruplex ligands examined in this study is more extensive than previous studies with RecQ helicases. However, comparing those ligands that have also been studied for RecQ-family G-quadruplex DNA helicase inhibition reveals examples of RecQ-family G-quadruplex helicase inhibitors that are not T-ag G-quadruplex DNA helicase inhibitors (TMPyP4) or are much less effective inhibitors of T-ag (NMM), as well as a T-ag G-quadruplex DNA helicase inhibitor that does not inhibit recQ helicases (distamycin A). One complicating factor in making these comparisons is the different types and sequences of G-quadruplex DNA that have been employed in previous helicase inhibition studies. However, given the lack of selectivity of the previous agents for particular G-quadruplex sequences, the comparisons are still informa-

tive. These differences provide evidence that the mode of interaction of RecQ helicases through their RQC domains with G-quadruplex DNA is distinct from the interaction of T-ag with G-quadruplex DNA substrates.

PDIs Are Potent and Selective Inhibitors of T-ag G-Quadruplex Helicase Activity. In addition to the G-quadruplex DNA ligands examined previously, the T-ag G-quadruplex DNA helicase inhibition due to a series of PDIs was also investigated. In T-ag G-quadruplex DNA helicase assays, the PDI Tel11 is a very effective inhibitor, completely preventing the unwinding of G′2-DNA at 10 μM concentration (Figure 6). Other PDIs, including PIPER and Tel01, are also very potent inhibitors of the G-quadruplex helicase activity of T-ag, with submicromolar IC_{50} values, similar to Tel11 (Table 1). These three PDIs are the most potent inhibitors of the G-quadruplex helicase activity of T-ag of all of the G-quadruplex DNA ligands examined here. One of these PDIs, PIPER, was also previously shown to be a potent inhibitor of the G-quadruplex DNA unwinding activity of Sgs1p (*44*).

While both Tel01 and PIPER have been shown to undergo pH-dependent aggregation in aqueous solutions, Tel11, which bears constitutively positively charged side chains, has a reduced propensity for self-association. Tel12, with anionic phosphonate side chains, also has a reduced propensity for self-association as compared to Tel01 and PIPER but is only a weak inhibitor of the G-quadruplex DNA helicase activity of T-ag (Table 1). Tel18 and Tel34, cationic PDIs with modified chromophores, are more active than Tel12 but much less effective inhibitors as compared to Tel11, despite the presence of identical side chains in these cationic PDIs (Table 1).

The ability of certain PDIs to inhibit the G-quadruplex helicase activity of T-ag is striking when compared to other G-quadruplex-interactive agents. Those PDIs bearing basic or constitutively cationic side chains are particularly effective inhibitors, indicating that electrostatic interaction with the G-quadruplex DNA may play an important role in preventing access by T-ag. Both Tel01 and PIPER have been shown to facilitate the formation of G-quadruplex DNA from single-stranded DNA, and a possible role for this in the apparent inhibition of the T-ag G-quadruplex DNA helicase observed here was examined. Incubation of partially annealed G′2-DNA1 with PIPER or Tel01 under the helicase assay conditions did not result in the formation of additional G-quadruplex DNA (data not shown). This indicates that these PDIs do not act by facilitating the reannealing of G-quadruplex DNA from single-stranded DNA formed by T-ag helicase activity in these assays but rather by inhibiting the formation of these single-stranded DNA products.

The ability of these PDIs to inhibit the duplex DNA helicase activity of T-ag was also investigated. In the presence of higher concentrations of T-ag than employed for the bimolecular quadruplex unwinding assays, T-ag can unwind duplex DNA2/3 by approximately 50% in the absence of inhibitor (Figure 7). In the presence of Tel11, which is a potent inhibitor of the G-quadruplex unwinding activity of T-ag, the duplex helicase activity is only moderately inhibited (Figure 7). Tel11 is a selective G-quadruplex helicase inhibitor; there is an approximately 500-fold difference in the concentrations required for G-quadruplex versus duplex helicase inhibition by Tel11. When these duplex unwinding assays were carried out under identical conditions as those employed to assay the bimolecular G-quadruplex unwinding inhibition, where the uninhibited extent of duplex unwinding was only ~12%, similar results were obtained (Supporting Information). When Tel01 and PIPER were assayed under these conditions, they demonstrated no inhibition of the duplex unwinding activity of T-ag at concentrations as high as 100 μM (Supporting Information). This lack of inhibition of the duplex helicase activity of T-ag by Tel01 and PIPER under an identical enzyme concentration as the bimolecular G-quadruplex helicase assays demonstrates that their potent G-quadruplex helicase inhibition is not simply due to ligand aggregation. Shoichet and co-workers have shown that ligand aggregation can lead to nonspecific inhibition of a wide range of enzymes (*69*). If these PDIs were inhibiting T-ag through aggregation-mediated sequestration of the enzyme, they would be equally effective in preventing the unwinding of both substrates. In fact, Tel01 undergoes aggregation under the helicase assay conditions as evidenced by a lack of Tel01 fluorescence, distinctive red-shift and hypochromicity in the Tel01 absorbance spectrum, and a distinctive resonance light-scattering signal (see Supporting Information). Previous studies have demonstrated that aggregation of PDIs is correlated with an increased binding selectivity for G-quadruplex DNA (*37*, *38*). The selective inhibition of the G-quadruplex helicase activity of T-ag by aggregating PDIs such as Tel01 may reflect this binding selectivity for G-quadruplex DNA. However, in this case, the aggregates do not interact directly with the helicase, as evidenced by the lack of inhibition of the duplex unwinding activity.

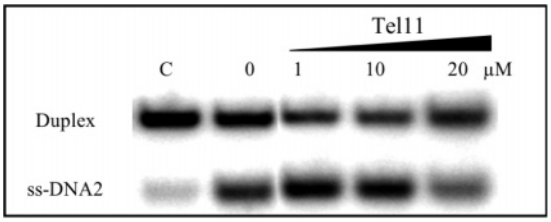

FIGURE 7: Inhibition of the duplex DNA helicase activity of T-ag by a representative G-quadruplex-interactive agent. Tel11 was incubated with 5′-labeled ds-DNA2/3 in helicase buffer for 60 min prior to the addition of 0.8 μg of recombinant, immunopurified T-ag and 4 mM ATP. After 90 min at 37 °C, the reactions were stopped, and the products were analyzed by nondenaturing gel electrophoresis. Lanes are labeled with the final concentration of ligand. The control lane C is DNA in the absence of both ligand and T-ag, and lane 0 is DNA in the presence of T-ag and ATP with no added ligand.

SPR Analysis of the G-Quadruplex Binding of T-ag Inhibitory and Noninhibitory Ligands Reveals Differences in Binding Affinity and Kinetics. The selectivity for inhibiting T-ag G-quadruplex DNA helicase activity versus duplex DNA helicase activity demonstrated by Tel01, PIPER, Tel11, and NMM provides strong evidence that these inhibitors act by binding to the G-quadruplex DNA substrate, preventing its unwinding by T-ag, as opposed to binding to T-ag. To gain more insight into the G-quadruplex DNA binding characteristics that may be involved in effective T-ag G-quadruplex helicase inhibition, the binding of two representative ligands to intramolecular G-quadruplex DNA was examined using surface plasmon resonance.

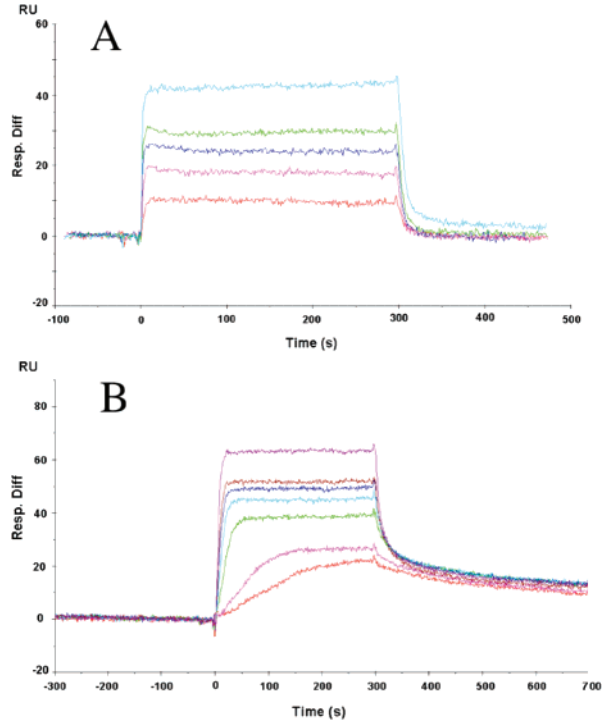

FIGURE 8: SPR sensorgrams for the interaction of TMPyP4 (A) and Tel11 (B) with the human telomeric intramolecular G-quadruplex. The concentrations of TMPyP4 are 50, 150, 300, 450, and 1350 nM, respectively, from bottom to top. Concentrations of Tel11 solutions are 5, 10, 50, 100, 150, 200, and 350 nM, respectively, from bottom to top. Experiments were conducted at 25 °C in HBS-EP buffer containing 200 mM K^+.

Although TMPyP4 does not inhibit the G-quadruplex unwinding activity of T-ag, a fast on and off rate for the binding of this ligand to the intramolecular human telomeric sequence 5′-biotinylated $(TTAGGG)_4TT$ is evident in the SPR analysis shown in Figure 8. After injection of a TMPyP4 flow solution across the immobilized G-quadruplex DNA, binding reached a steady-state equilibrium almost immediately at all concentrations employed. Similarly, at the end of the injection, TMPyP4 dissociated rapidly from the DNA substrate when the flow solution was replaced with running buffer. The observed RU in the steady-state region was plotted against the concentration of TMPyP4 to calculate a steady-state equilibrium binding constant ($K_A = 6.04 \times 10^6$ M^{-1} and $K_D = 0.17$ μM). Kinetic k_{on} and k_{off} values were determined using the 1:1 Langmuir binding model in the BIAevaluation software (1.24×10^6 M^{-1} s^{-1} and 0.155 s^{-1}, respectively; fitting of binding curves is shown in the Supporting Information).

In contrast, the binding of Tel11 to the same G-quadruplex sequence exhibits different kinetic characteristics (Figure 8). Most notably, although an initial fast dissociation was observed at higher concentrations of Tel11, at all concentrations, the majority of the dissociation phase appeared to be much slower than that of TMPyP4. In fact, fitting of the k_{off} rate was complicated by the observed dissociation behavior. Fitting of k_{off} separately from k_{on} in the BIAevaluation software beginning 74 s after the start of dissociation gave a value of 1.36×10^{-3} s^{-1} at all concentrations of Tel11. This observed off rate is 2 orders of magnitude slower than the dissociation of TMPyP4 from the same DNA substrate. In addition, at lower concentrations of Tel11, binding does not reach equilibrium as quickly as seen for TMPyP4. The observed kinetic behavior may reflect the presence of two different binding modes for Tel11: one tight, high-affinity mode reflected in the overall slow dissociation observed and a second nonspecific mode of binding observed more readily at higher concentrations of Tel11. The binding response in the steady-state region does not fit well to a 1:1 binding site model, in agreement with results obtained by fluorescence titrations of Tel11 with G′2-DNA1.

DNA Binding Affinity Alone Does Not Lead to T-ag Helicase Inhibition. To provide further insights into the duplex- and G-quadruplex DNA binding factors that give rise to potent T-ag helicase inhibition by these ligands, the interaction of representative inhibitors with the G′2-DNA1 and ds-DNA2/3 substrates was determined by fluorescence titration in the helicase buffer. Examples of selective (NMM and Tel11), nonselective (Tel12), and inactive (TMPyP4) G-quadruplex helicase inhibitors that display changes in fluorescence upon DNA addition under the helicase assay conditions were employed for these studies.

Titrations of a solution of NMM (1 μM) with G′2-DNA1 and ds-DNA2/3 (Figure 9A) in helicase buffer demonstrate the previously reported G-quadruplex DNA-specific increase in the fluorescence of this ligand (*70*). Nonlinear least-squares fitting of the observed fluorescence increase to a simple equilibrium binding model (*45*) affords a dissociation constant for NMM binding to this G-quadruplex DNA of 0.09 ± 0.04 μM and a binding site size of 0.44 ± 0.04 quadruplex (Table 2). The apparent stoichiometry of one NMM to two quadruplexes has precedent in the previously reported ability of end-stacking ligands such as PIPER to bridge two G-quadruplexes (*31*). The lack of fluorescence change upon the addition of ds-DNA2/3 to NMM leads to a lower limit for the dissociation constant for the NMM-duplex DNA complex of 50 μM. The binding selectivity of NMM for G′2-DNA1 revealed in these titrations is reflected in the selectivity for G-quadruplex DNA helicase inhibition by NMM in the T-ag assays (Table 1 and Supporting Information).

Similar fluorescence titrations carried out with TMPyP4 displayed a more complex behavior (Figure 9B). Addition of either G′2-DNA1 or ds-DNA2/3 to solutions of TMPyP4 (1 μM) caused an initial decrease of ligand fluorescence that was only observed at very low concentrations of added DNA. In the presence of higher concentrations of DNA, the ligand fluorescence increased. Both G′2-DNA1 and ds-DNA2/3 have single-stranded DNA tails, and the initial fluorescence quenching observed for these two DNA structures may be due to single-strand DNA-mediated aggregation of this ligand, as has been seen for related cationic porphyrins (*71*). Because the T-ag unwinding of these two DNA substrates is differentially inhibited by TMPyP4, this putative single-stranded DNA interaction with TMPyP4 cannot be the origin of the helicase inhibition. Fitting the portion of the titration curve associated with the G-quadruplex- or duplex-DNA-mediated fluorescence increase (*70*) affords apparent dissociation constants of 1.0 and 0.19 μM, respectively (Table 2). This binding preference of TMPyP4 for the duplex DNA helicase substrate is in accord with the selective inhibition of the duplex helicase activity of T-ag displayed by this porphyrin (Supporting Information).

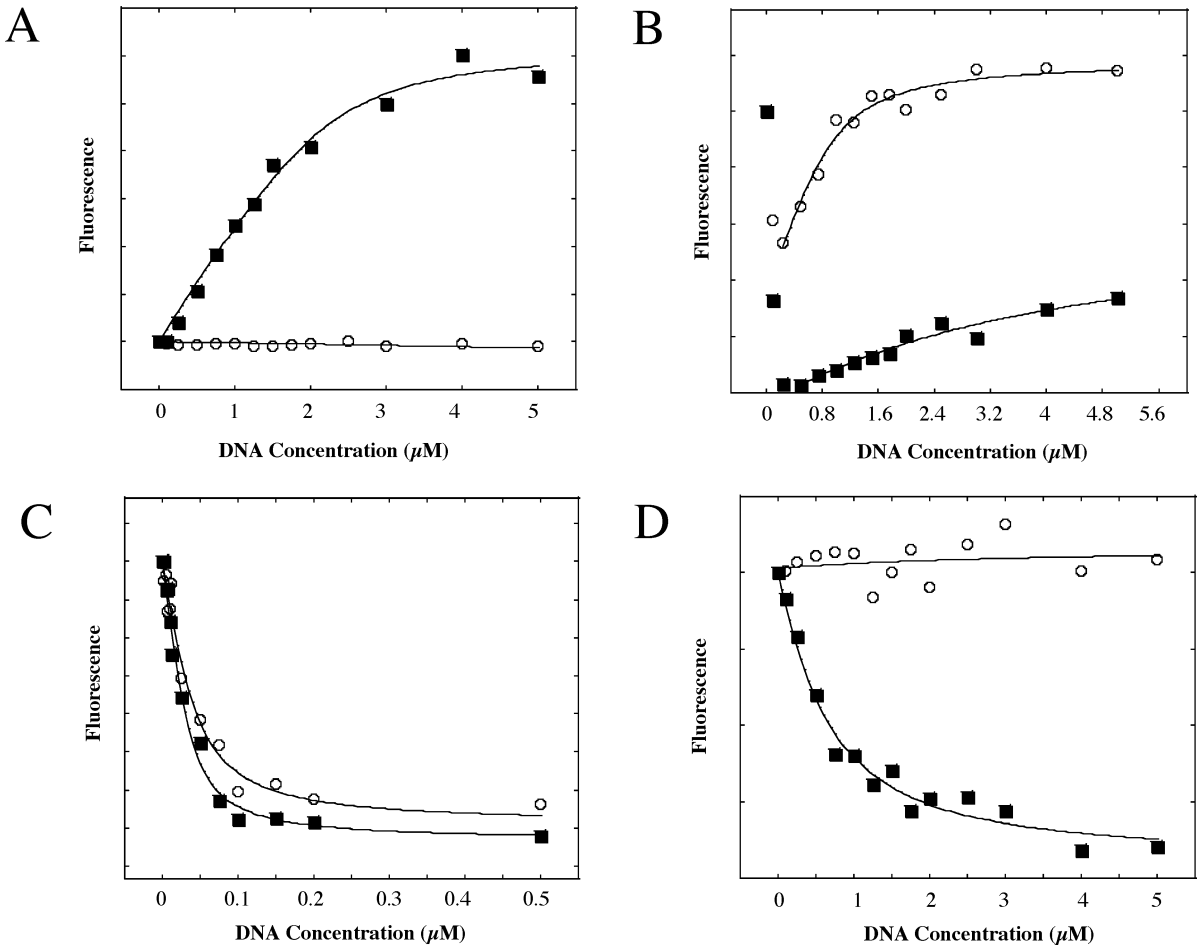

FIGURE 9: G-quadruplex- and duplex-DNA binding by selected G-quadruplex-interactive agents determined by fluorescence titrations with ds-DNA2/3 and G′2-DNA1 in helicase reaction buffer. The ligands NMM (A), TMPyP4 (B), Tel11 (C), and Tel12 (D) (1 μM) and various concentrations of G′2-DNA (solid squares) or ds-DNA2/3 (open circles) were mixed in buffer containing 10 mM Tris-HCl buffer (pH 7), 10 mM KCl, 10 mM $MgCl_2$, 0.5 mM 1,4-dithiothreitol, 0.1 mM EDTA, and 10% glycerol. The solutions were allowed to equilibrate, and their fluorescence was measured. The curves represent the nonlinear least-squares fits of the data to the quadratic binding equation.

Table 2: G-Quadruplex and Duplex DNA Binding by G-Quadruplex-Interactive SV40 T-ag Inhibitors

compound	K_d G2-DNA1[a] (binding site size)[b] (μM)	K_d ds-DNA2/3[a] (binding site size) (μM)
NMM	0.09 ± 0.04 ($n = 0.44 \pm 0.04$)	NB[c]
TMPyP4	1.0 ± 0.9 ($n = 0.44 \pm 0.25$)	0.19 ± 0.08 ($n = 1.1 \pm 0.2$)
Tel11	0.27 ± 0.11 ($n = 28 \pm 5$)	0.43 ± 0.25 ($n = 26 \pm 8$)
Tel12	0.95 ± 0.60 ($n = 2.3 \pm 1.1$)	NB[c]

[a] Determined by fluorescence titration of G′2-DNA or ds-DNA2/3 into solutions of ligands (1 μM) in helicase buffer (10 mM Tris (pH 7), 10 mM KCl, 10 mM $MgCl_2$, 0.5 mM 1,4-dithiothreitol, 0.5 mM EDTA, 10% glycerol). Dissociation constants were determined by nonlinear least-squares fitting of the increase or decrease of fluorescence due to ligand binding to DNA as described in the Experimental Procedures. [b] Expressed as the ratio of ligand to DNA structure. [c] No binding was observed in the presence of up to a 5-fold excess of DNA.

The fluorescence due to solutions of Tel11 (1 μM) was quenched upon addition of either G′2-DNA1 or ds-DNA2/3 (Figure 9C), similar to what has been reported earlier for this ligand (*38*). This quenching occurs at concentrations of DNA well below that of the ligand, indicating that multiple ligands bind to each DNA structure, which is also similar to what was observed previously (*38*). Fitting the fluorescence data to a simple multisite binding model (*45*) resulted in a calculated dissociation constant of 0.27 ± 0.11 μM with 28 $\pm$ 5 binding sites per G′2-DNA1. The dissociation constant for ds-DNA2/3 is only slightly higher, 0.42 ± 0.60 μM, with 25 $\pm$ 8 binding sites per DNA. In contrast to the approximately 400-fold selectivity exhibited by Tel11 for G-quadruplex versus duplex DNA helicase inhibition, this PDI displays less than a 2-fold binding preference for the G-quadruplex DNA substrate (Table 2).

The anionic Tel12 also undergoes fluorescence quenching in the presence of the G′2-DNA substrate; however, upon addition of ds-DNA2/3, very little change in fluorescence is observed (Figure 9D). The increased selectivity for G-quadruplex DNA binding by Tel12 as compared to Tel11 has been noted (*36*). The dissociation constant for G′2-DNA1 binding by Tel12 (0.95 ± 0.60 μM) is a least 50-fold lower than that for ds-DNA2/3, for which a lower limit of 50 μM is estimated (Table 2). Despite this high level of G-quadruplex DNA binding selectivity, Tel12 does not selectively inhibit the G-quadruplex DNA unwinding activity of T-ag (Table 1 and Supporting Information). While the inhibitory effects of Tel12 on the G-quadruplex helicase activity of T-ag can be understood on the basis of its association with the G-quadruplex DNA substrate, the origin of the duplex helicase inhibition is not clear.

These DNA binding data reveal that factors in addition to binding affinity for the substrate DNA play a role in effective T-ag helicase inhibition. The binding affinities for the

G-quadruplex DNA helicase substrate of these four ligands differ by only a factor of 10, yet the helicase inhibitory potency for these ligands ranges from very potent (submicromolar IC_{50}) to inactive. The interaction of Tel12 with G-quadruplex DNA, although similar in affinity to that for TMPyP4, is more effective in preventing T-ag unwinding than that of TMPyP4. The large difference in T-ag G-quadruplex DNA helicase inhibition between the anionic PDI Tel12 and the cationic PDI Tel11 is not reflected in a similarly large difference in binding affinity for these two ligands to the DNA substrate.

The precise requirements for effective inhibition of the quadruplex helicase activity of T-ag by G-quadruplex-interactive compounds remain unclear. The previously reported observation that certain GROs inhibit the duplex helicase activity of T-ag (*28*) may be due to the G-quadruplex structures of these GROs binding tightly to T-ag and preventing helicase activity. In this scenario, G-quadruplex ligands that bind to and facilitate this interaction of quadruplex structures and T-ag would be more effective inhibitors than ligands whose binding to G-quadruplex structures inhibits T-ag binding. This is similar to the case reported for NMM inhibition of BLM, in which NMM binding to quadruplex DNA does not inhibit BLM binding but rather serves to stabilize the interaction and prevent both dissociation and translocation (*41*). However, NMM is only a modest inhibitor of the quadruplex unwinding by T-ag, and this could be due to differences in the way that these two different helicases interact with G-quadruplex DNA or to a different means of inhibition by G-quadruplex ligands in the case of T-ag. T-ag lacks the RQC domain that is responsible for G-quadruplex DNA binding by RecQ-family helicases such as BLM, and so it is quite likely that the specific interactions made between T-ag and quadruplex DNA are different from those of RecQ helicases. On the other hand, those ligands that inhibit the quadruplex helicase activity of T-ag most strongly, the PDIs Tel01, PIPIER, and Tel11, share an ability to bind to G-quadruplex DNA with high stoichiometry, indicating that this is an important feature for T-ag inhibition that is different from the model for RecQ helicase inhibition by NMM.

There is a growing interest in G-quadruplex DNA-interactive agents as potential telomere- and telomerase-targeting agents (*1*, *72*−*74*) or transcriptional regulators (*75*−*79*), although no such agents have been clinically proven. Proposed therapeutic approaches involving G-quadruplex-interactive agents require selective targeting, not only of G-quadruplex structures but also of specific G-quadruplex-associated proteins. The demonstration of T-ag quadruplex helicase inhibition by certain G-quadruplex-interactive agents indicates that helicases must be considered as potential targets of these compounds. As different families of G-quadruplex helicases may interact differently with their substrates, certain types of G-quadruplex ligands may be better inhibitors of specific helicase families.

CONCLUSION

Previous reports of G-quadruplex helicase activity have focused on the RecQ family of helicases. While not all DNA helicases have the ability to unwind G-quadruplex DNA structures, SV40 T-ag does have this ability. The demonstration that the duplex and G-quadruplex unwinding activity of T-ag are comparable, along with the identification of sequences that may adopt a G-quadruplex conformation in the SV40 genome, indicate that hexameric, replicative helicases may play a role in resolving G-quadruplex DNA structures during DNA replication. The mechanism by which hexameric helicases unwind G-quadruplex DNA is not known; however, it is distinct from that employed by the RecQ helicases. The interaction of T-ag with G-quadruplex DNA substrates is different from that of the RecQ helicases, which involve a conserved RQC domain. T-ag does not contain a RQC domain or any other protein domain previously identified as a G-quadruplex DNA binding motif. These differences between the RecQ helicases and T-ag are reflected in the different types of G-quadruplex-interactive ligands that inhibit these two distinct families of G-quadruplex helicases. Studies of the T-ag G-quadruplex helicase inhibition by a range of G-quadruplex-interactive agents indicates that binding affinity alone does not predict effective helicase inhibition. Specific binding interactions with the substrate DNA may be more effective in preventing access to or processing of the DNA substrate as compared to other binding interactions, and these may vary from one family of G-quadruplex helicases to another. Additional factors, such as the kinetics of dissociation of the ligand-G-quadruplex complex and the binding stoichiometry of these G-quadruplex ligands, may also play a role in effective helicase inhibition. PDI Tel11, identified as the most potent inhibitor of the G-quadruplex helicase activity of T-ag, binds to the substrate DNA with high stoichiometry and dissociates slowly from the complex formed with an intramolecular G-quadruplex. Interestingly, despite a relative lack of selectivity in binding to the G-quadruplex versus the duplex DNA substrate, Tel11 is highly selective for inhibiting the G-quadruplex helicase activity of T-ag; the duplex helicase activity is only inhibited at concentrations of Tel11 400-fold higher than those required to inhibit the quadruplex helicase activity. The identification of potent and selective inhibitors of the G-quadruplex helicase activity of T-ag provides tools for probing the specific role of this activity in SV40 replication. These studies may lead to new insights into the role of G-quadruplex structures in DNA replication and may ultimately allow the targeting of these structures in the design of highly selective inhibitors of viral replication.

ACKNOWLEDGMENT

Prof. Daniel Simmons, University of Delaware, is gratefully acknowledged for providing immunochromatography-purified recombinant T-ag.

SUPPORTING INFORMATION AVAILABLE

Synthetic details, PAGE gels, table of QGRS in SV40, DMS protection gels, and SPR kinetic fits. This material is available free of charge via the Internet at http://pubs.acs.org.

REFERENCES

1. Kerwin, S. M. (2000) G-Quadruplex DNA as a target for drug design, *Curr. Pharm. Des. 6*, 441−471.
2. Kan, Z. Y., Yao, Y. A., Wang, P., Li, X. H., Hao, Y. H., and Tan, Z. (2006) Molecular crowding induces telomere G-quadruplex formation under salt-deficient conditions and enhances its competition with duplex formation, *Angew. Chem., Int. Ed. 45*, 1629−1632.

3. Phan, A. T., and Mergny, J. L. (2002) Human telomeric DNA: G-quadruplex, i-motif, and Watson−Crick double helix, *Nucleic Acids Res. 30*, 4618−4625
4. Li, W., Miyoshi, D., Nakano, S., and Sugimoto, N. (2003) Structural competition involving G-quadruplex DNA and its complement, *Biochemistry 42*, 11736−11744.
5. Davis, J. T. (2004) G-quartets 40 years later: From 5′-GMP to molecular biology and supramolecular chemistry, *Angew. Chem., Int. Ed. 43*, 668−698.
6. Huppert, J. L., and Balasubramanian, S. (2005) Prevalence of quadruplexes in the human genome, *Nucleic Acids Res. 33*, 2908−2916.
7. Todd, A. K., Johnston, M., and Neidle, S. (2005) Highly prevalent putative quadruplex sequence motifs in human DNA, *Nucleic Acids Res. 33*, 2901−2907.
8. Duquette, M. L., Huber, M. D., and Maizels, N. (2007) G-rich proto-oncogenes are targeted for genomic instability in B-cell lymphomas, *Cancer Res. 67*, 2586−2594.
9. Fry, M., and Leob, L. A. (1994) The fragile X syndrome d(CGG)-*n* nucleotide repeats form a stable tetrahelical structure, *Proc. Natl. Acad. Sci. U.S.A. 91*, 4950−4954.
10. Saha, T., and Usdin, K. (2001) Tetraplex formation by the progressive myoclonus epilepsy type-1 repeat: Implications of instability in the repeat expansion diseases, *FEBS Lett. 491*, 184−187.
11. Eddy, J., Maizels, N. (2006) Gene function correlates with potential for G4 DNA formation in the human genome, *Nucleic Acids Res. 34*, 3887−3896.
12. Rawal, P., Kummarasetti, V. B. R., Ravindran, J., Kumar, N., Halder, K., Sharma, R., Mukerji, M., Das, S. K., and Chowdhury, S. (2006) Genome-wide prediction of G4 DNA as regulatory motifs: Role in *Escherichia coli* global regulation, *Genome Res.* 644−655.
13. Duquette, M. L., Handa, P., Vincent, J. A., Taylor, A. F., and Maizels, N. (2004) Intracellular transcription of G-rich DNA induces formation of G-quadruplex DNA structures in vivo, *Genes Dev. 18*, 1618−1629.
14. Oganesian, L., and Bryan, T. M. (2007) Physiological relevance of telomeric G-quadruplex formation: A potential drug target, *BioEssays 29*, 155−165.
15. Wu, X., and Maizels, N. (2001) Substrate-specific inhibition of RecQ helicase, *Nucleic Acids Res. 29*, 1765−1771.
16. Sun, H., Bennett, R. J., and Maizels, N. (1999) The *Saccharomyces cerevisiae* Sgs1 helicase efficiently unwinds G-G paired DNAs, *Nucleic Acids Res. 27*, 1978−1984.
17. Sun, H., Karow, J. K., Hickson, I. D., and Maizels, N. (1998) The Bloom's syndrome helicase unwinds G4 DNA, *J. Biol. Chem. 273*, 27587−27592.
18. Fry, M., and Loeb, L. A. (1999) Human Werner syndrome DNA helicase unwinds tetrahelical structures of the fragile X syndrome repeat sequence d(CGG)n, *J. Biol. Chem. 274*, 12797−12802.
19. Huber, M. D., Duquette, M. L., Shiels, J. C., and Maizels, N. (2006) A conserved G4 DNA binding domain in RecQ family helicases, *J. Mol. Biol. 358*, 1071−1080.
20. Vaughn, J. P., Creacy, S. D., Routh, E. D., Joyner-Butt, C., Jenkins, G. S., Pauli, S, Nagamine, Y., and Akman, S. A. (2005) The DEXH protein product of DHX36 gene is the major source of tetramolecular quadruplex G4-DNA resolving activity in HeLa cell lysates, *J. Biol. Chem. 280*, 38117−38120.
21. Simmons, D. T. (2000) SV40 large T antigen functions in DNA replication and transformation, *Adv. Virus Res. 55*, 75−133.
22. Li, J. J., and Kelly, T. J. (1984) Siman virus 40 DNA replication in vitro, *Proc. Natl. Acad. Sci. U.S.A. 81*, 6973−6977.
23. Dziegielewska, B., Kowalski, D., and Beerman, T. A. (2004) SV40 DNA replication inhibition by the monofunctional DNA alkylator Et743, *Biochemistry 43*, 14228−14237.
24. Bullock, P. A. (1997) The initiation of Simian Virus 40 DNA replication in vitro, *Crit. Rev. Biochem. Mol. Biol. 32*, 503−568.
25. Baran, N., Pucshansky, L., Marco, Y., Benjamin, S., and Manor, H. (1997) The SV40 large T-antigen helicase can unwind four stranded DNA structures linked by G-quartets, *Nucleic Acids Res. 25*, 297−303.
26. Patel, P. K., Bhavesh, N. S., and Hosur, R. V. (2000) NMR observation of a novel C-tetrad in the structure of the SV40 repeat sequence GGGCGG, *Biochem. Biophys. Res. Commun. 270*, 967−971.
27. Dapic, V., Abdomerovic, V., Marrington, R., Peberdy, J., Rodger, A., Trent, J. O., and Bates, P. J. (2003) Biophysical and biological properties of quadruplex oligodeoxyribonucleotides, *Nucleic Acids Res. 31*, 2097−2107.
28. Xu, X., Hamhouyia, F., Thomas, S. D., Burke, T. J., Girvan, A. C., McGregor, W. G., Trent, J. O., Miller, D. M., and Bates, P. J. (2001) Inhibition of DNA replication and induction of S phase cell cycle arrest by G-rich oligonucleotides, *J. Biol. Chem. 276*, 43221−43230.
29. Hardin, C. C., Perry, A. G., and White, K. (2001) Thermodynamics and kinetic characterization of the dissociation and assembly of quadruplex nucleic acids, *Biopolymers 56*, 147−194.
30. Han, H. Y., Hurley, L. H., and Salazar, M. (1999) A DNA polymerase stop assay for G-quadruplex-interactive compounds, *Nucleic Acids Res. 27*, 537−542.
31. Fedoroff, O. Y., Salazar, M., Han, H. Y., Chemeris, V. V., Kerwin, S. M., and Hurley, L. H. (1998) NMR model of a telomerase-inhibiting compound bound to G-quadruplex DNA, *Biochemistry 37*, 12367−12374.
32. Kern, J. T., and Kerwin, S. M. (2002) The aggregation and G-quadruplex DNA selectivity of charged 3,4,9,10-perylenetetracarboxylic acid diimides, *Bioorg. Med. Chem. Lett. 12*, 3395−3398.
33. Tuntiwechapikul, W., and Salazar, M. (2001) Cleavage of telomeric G-quadruplex DNA with perylene-EDTA-Fe(II), *Biochemistry 40*, 13652−13658.
34. Rossetti, L., Franceschin, M., Schirripa, S., Bianco, A., Ortaggi, G., and Savino, M. (2005) Selective interactions of perylene derivatives having different side chains with inter- and intramolecular G-quadruplex DNA structures. A correlation with telomerase inhibition, *Bioorg. Med Chem. Lett. 15*, 413−420.
35. Tuntiwechapikul, W., Taka, T., Bethencourt, M., Makonkawkeyoon, L., and Lee, T. R. (2006) The influence of pH on the G-quadruplex binding selectivity of perylene derivatives, *Bioorg. Med. Chem. Lett. 16*, 4120−4126.
36. Samudrala, R., Zhang, X., Wadkins, R. M., and Mattern, D. L. (2007) Synthesis of a non-cationic, water-soluble perylenetetracarboxylic diimide and its interactions with G-quadruplex-forming DNA, *Bioorg. Med. Chem. 15*, 186−193.
37. Sissi, C., Lucatello, L., Krapcho, A. P., Maloney, D. J., Boxer, M. B., Camarasa, M. V., Pezzoni, G., Menta, E., and Palumbo, M. (2007) Tri-, tetra-, and heptacyclic perylene analogues as new potential antineoplastic agents based on DNA telomerase inhibition, *Bioorg. Med. Chem. 15*, 555−562.
38. Kern, J. T., Thomas, P. W., and Kerwin, S. M. (2002) The relationship between ligand aggregation and G-quadruplex DNA selectivity in a series of 3,4,9,10-perylenetetracarboxylic acid diimides, *Biochemistry 41*, 11379−11389.
39. David, W. M., Brodbelt, J., Kerwin, S. M., and Thomas, P. W. (2002) Investigation of quadruplex oligonucleotide−drug interactions by electrospray ionization-mass spectrometry, *Anal. Chem. 74*, 2029−2033.
40. Gupta, R., and Brosh, R. M., Jr. (2007) DNA repair helicases as targets for anti-cancer therapy, *Curr. Med. Chem. 14*, 503−517.
41. Huber, M. D., Lee, D. C., and Maizels, N. (2002) G4 DNA unwinding by Blm and Sgs1p: Substrate specificity and substrate-specific inhibition, *Nucleic Acids Res. 30*, 3954−3961.
42. Li, J. L., Harrison, R. J., Reszka, A. P., Brosh, R. M., Bohr, V. A., Neidle, S., and Hickson, I. D. (2001) Inhibition of the Bloom's and Werner's syndrome helicases by G-quadruplex interacting ligands, *Biochemistry 40*, 15194−15202.
43. Cocco, M. J., Hanakahi, L. A., Huber, M. D., and Maizels, N. (2003) Specific interactions of distamycin with G-quadruplex DNA, *Nucleic Acids Res. 31*, 2944−2951.
44. Han, H. Y., Bennett, R. J., and Hurley, L. H. (2000) Inhibition of unwinding of G-quadruplex structures by Sgs1 helicase in the presence of *N,N*′-bis[2-(1-piperidino)ethyl]-3,4,9,10-perylenetetracarboxylic diimide, a G-quadruplex-interactive ligand, *Biochemistry 39*, 9311−9316.
45. Stootman, F. H., Fisher, D. M., Rodger, A., and Aldrich-Wright, J. R. (2006) Improved curve fitting procedures to determine equilibrium binding constants, *Analyst 131*, 1145−1151.
46. Mazzitelli, C. L., Rodriguez, M., Kern, J. T., Kerwin, S. M., and Brodbelt, J. S. (2006) Evaluation of binding of perylene diimide and benzannulated perylene diimide ligands to DNA by electrospray ionization mass spectrometry, *J. Am. Soc. Mass Spectrom. 17*, 593−604.
47. Franceschin, M., Alvino, A., Casagrande, V., Mauriello, C., Pascucci, E., Savino, M., Ortaggi, G., and Bianco, A. (2007) Specific interactions with intra- and intermolecular G-quadruplex

DNA structures by hydrosoluble coronene derivatives: A new class of telomerase inhibitors, *Bioorg. Med. Chem. 15*, 1848−1858.
48. Sadrai, M., Hadel, L., Sauers, R. R., Husain, S., Krogh-Jespersen, K., Westbrook, J. D., and Bird, G. R. (1992) Lasing action in a family of perylene derivatives: Singlet absorption and emission spectra, triplet absorption and oxygen quenching constants, and molecular mechanics and semiempirical molecular-orbital calculations, *J. Phys. Chem. 96*, 7988−7996.
49. Molecular mechanics calculations were carried out to confirm the prediction that the twisted chromophore of Tel18, particularly the (M)-enantiomer, could still effectively interact with the terminal G-tetrads of G-quadruplex DNA.
50. Langhals, H., and Kirner, S. (2000) Novel fluorescent dyes by the extension of the core of perylenetetracarboxylic bisimides, *Eur. J. Org. Chem.* 365−380.
51. This is not the case with appropriate intramolecular G-quadruplex helicase substrates with 3′-tails, which are not well-resolved from single-stranded DNA on nondenaturing PAGE (data not shown).
52. Immunochromatography-purified recombinant T-ag expressed in Sf9 insect cells was kindly provided by Prof. Daniel Simmons, University of Delaware, and was prepared according to: Simmons, D. T., Melendy, T., Usher, D., and Stillman, D. (1996) Simian virus 40 large T antigen binds to topoisomerase I, *Virology 222*, 365−374.
53. Kouzine, F., and Levens, D. (2007) Supercoil-driven DNA structures regulate genetic transactions, *Front. Biosci. 12*, 4409−4423
54. Scaria, V., Hariharan, M., Arora, A., Maiti, S., Kikin, O., D'Antonio, L., and Bagga, P. S. (2006) Quadfinder: Server for identification and analysis of quadruplex-forming motifs in nucleotide sequences, *Nucleic Acids Res. 34*, 683−685.
55. Kikin, O., D'Antonio, L., and Bagga, P. (2006) SQGRS Mapper: A web-based server for predicting G-quadruplexes in nucleotide sequences, *Nucleic Acids Res. 34*, 676−682.
56. Lednicky, J., and Folk, W. R. (1992) Two synthetic Sp1-binding sites functional substitute for the 21-base-pair repeat region to activate simian virus growth in CV-1 cells, *J. Virol. 66*, 6379−6390.
57. Han, H., Langley, D. R., Rangan, A., and Hurley, L. H. (2001) Selective interactions of cationic porphyrins with G-quadruplex structures, *J. Am. Chem. Soc. 123*, 8902−8913.
58. Chen, Q., Kuntz, I. D., and Shafer, R. H. (1996) Spectroscopic recognition of guanine dimeric hairpin quadruplexes by a carbocyanine dye, *Proc. Natl. Acad. Sci. U.S.A. 93*, 2635−2639.
59. Cheng, J.-Y., Lin, S.-H., and Chang, T.-C. (1998) Vibrational investigation of DODC cation for recognition of guanine dimeric hairpin quadruplex studied by satellite holes, *J. Phys. Chem. B 102*, 5542−5546.
60. Franceschin, M., Rossetti, L., D'Ambrosio, A., Schirripa, S., Bianco, A., Ortaggi, G., Savino, M., Schultes, C., and Neidle, S. (2006) Natural and synthetic G-quadruplex interactive berberine derivatives, *Bioorg. Med. Chem. Lett. 16*, 1707−1711.
61. Maiti, S., Chaudhury, N. K., and Chowdhury, S. (2003) Hoechst 33258 binds to G-quadruplex in the promoter region of human *c*-myc, *Biochem. Biophys. Res. Commun. 310*, 505−512.
62. Kerwin, S. M., Sun, D., Kern, J. T., Rangan, A., and Thomas, P. W. (2001) G-quadruplex DNA binding by a series of carbocyanine dyes, *Bioorg. Med. Chem. Lett. 11*, 2411−2414.
63. Brosh, R. M., Jr., Karow, J. K., White, E. J., Shaw, N. D., Hickson, I. D., and Bohr, V. A. (2000) Potent inhibition of Werner and Bloom helicases by DNA minor groove binding drugs, *Nucleic Acids Res. 28*, 2420−2430.
64. Pothukuchy, A., Mazzitelli, C. L., Rodriguez, M. L., Tuesuwan, B., Salazar, M., Brodbelt, J. S., and Kerwin, S. M. (2005) Duplex and quadruplex DNA binding and photocleavage by trioxatriangulenium ion, *Biochemistry 44*, 2163−2172.
65. Guo, Q., Lu, M., Marky, L. A., and Kallenbach, N. R. (1992) Interaction of the dye ethidium bromide with DNA containing guanine repeats, *Biochemistry 31*, 2451−2455.
66. Rosu, F., De Pauw, E., Guittat, L., Alberti, P., Lacroix, L., Mailliet, P., Riou, J.-F., and Mergny, J.-L. (2003) Selective interaction of ethidium derivatives with quadruplexes: An equilibrium dialysis and electrospray ionization mass spectrometry analysis, *Biochemistry 42*, 10361−10371.
67. Bachur, N. R., Yu, F., Johnson, R., Hickey, R., Wu, Y., and Malkas, L. (1992) Helicase inhibition by anthracycline anticancer agents, *Mol. Pharmacol. 41*, 993−998.
68. Randazzo, A., Galeone, A., and Mayol, L. (2001) ^{1}H NMR study of the interaction of distamycin A and netropsin with the parallel stranded tetraplex [d(TGGGGT)]$_4$, *Chem. Commun. 11*, 1030−1031.
69. McGovern, S. L., Helfand, B. T., Feng, B., and Shoichet, B. K. (2003) A specific mechanism of nonspecific inhibition, *J. Med. Chem. 46*, 4265−4272.
70. Arthanari, H., Basu, S., Kawano, T. L., and Bolton, P. H. (1998) Fluorescent dyes specific for quadruplex DNA, *Nucleic Acids Res. 26*, 3724−3728.
71. Pasternack, R. F., Goldsmith, J. I., Szep, S., and Gibbs, E. J. (1998) A spectroscopic and thermodynamic study of porphyrin/DNA supramolecular assemblies, *Biophys. J. 75*, 1024−1031.
72. Raymond, E., Soria, J.-C., Izbicka, E., Boussin, F., Hurley, L., and Von Hoff, D. D. (2000) DNA G-quadruplexes, telomere-specific proteins, and telomere-associated enzymes as potential targets for new anticancer drugs, *Invest. New Drugs 18*, 123−137.
73. Neidle, S., and Parkinson, G. (2002) Telomere maintenance as a target for anticancer drug discovery, *Nat. Rev. Drug Discov. 1*, 383−393.
74. Shay, J. W., and Wright, W. E. (2006) Telomerase therapeutics for cancer: Challenges and new directions, *Nat. Rev. Drug Discov. 5*, 577−584.
75. Hurley, L. H. (2001) Secondary DNA structures as molecular targets for cancer therapeutics, *Biochem. Soc. Trans. 29*, 692−696.
76. Sun, D., Guo, K., Rusche, J. J., and Hurley, L. H. (2005) Facilitation of a structural transition in the polypurine/polypyrimidine tract within the proximal promoter region of the human VEGF gene by the presence of potassium and G-quadruplex-interactive agents, *Nucleic Acids Res. 33*, 6070−6080.
77. Rankin, S., Reszka, A. P., Huppert, J., Zloh, M., Parkinson, G. N., Todd, A. K., Ladame, S., Balasubramanian, S., and Neidle, S. (2005) Putative DNA quadruplex formation within the human *c*-kit oncogene, *J. Am. Chem. Soc. 127*, 10584−10589.
78. Siddiqui-Jain, A., Grand, C. L., Bearss, D. J., and Hurley, L. H. (2002) Direct evidence for a G-quadruplex in a promoter region and its targeting with a small molecule to repress *c*-MYC transcription, *Proc. Natl. Acad. Sci. U.S.A. 99*, 11593−11598.
79. Phan, A. T., Modi, Y. S., and Patel, D. J. (2004) Propeller-type parallel-stranded G-quadruplexes in the human *c*-myc promoter, *J. Am. Chem. Soc. 126*, 8710−8716.

BI701747D